

Cite this: *Dalton Trans.*, 2018, **47**, 5553Received 28th February 2018,  
Accepted 16th March 2018

DOI: 10.1039/c8dt00781k

rsc.li/dalton

## Cooperativity in spin crossover materials as ligand's responsibility – investigations of the Fe(II) – 1,3-bis((1*H*-tetrazol-1-yl)methyl)bicyclo[1.1.1]pentane system†

Christian Knoll,<sup>a</sup> Danny Müller,<sup>a</sup> Marco Seifried,<sup>a</sup> Gerald Giester,<sup>b</sup> Jan M. Welch,<sup>c</sup> Werner Artner,<sup>d</sup> Klaudia Hradil,<sup>d</sup> Michael Reissner<sup>e</sup> and Peter Weinberger<sup>a</sup>

**Criteria for a technologically relevant spin crossover (SCO) material include temperature and abruptness. A series of Fe(II) – 1,3-bis((1*H*-tetrazol-1-yl)methyl)bicyclo[1.1.1]pentane SCO complexes with various anions (BF<sub>4</sub><sup>−</sup>, ClO<sub>4</sub><sup>−</sup>, and PF<sub>6</sub><sup>−</sup>) designed using a structure–property based concept is reported. All complexes feature abrupt SCO-behavior with *T*<sub>1/2</sub> between 170 K and 187 K. These materials demonstrate that without stabilizing the effects of incorporated solvents or a hydrogen bond-network, the observed cooperativity during high-spin–low-spin transition is anion independent and originates only from the rigidity and internal strain of the propellane-moiety in the ligand. Spectroscopy and structural investigations of these materials are supported by quantum chemical calculations.**

Molecular bistability will be a key feature of the next generation of miniaturized magneto-optical devices.<sup>1,2</sup> In this context, the spin crossover (SCO) effect with its inherent change of magnetic moment,<sup>2,3</sup> color,<sup>4</sup> dielectric constant,<sup>5,6</sup> resistance,<sup>7–10</sup> conductivity<sup>7–11</sup> and molecular extension (bond-length)<sup>12</sup> upon an external stimulus such as light (LIESST-effect),<sup>13,14</sup> temperature,<sup>2,3</sup> pressure,<sup>2,3,15</sup> current,<sup>7–10</sup> *etc.*, allows for a multitude of attractive combinations of properties, guiding coordination and materials chemists alike. Application of such materials, however, requires different cri-

teria to be met by a suitable material. The most important of these characteristics includes an abrupt and complete spin crossover between the high-spin (HS) and the low-spin (LS) state, preferably at or near ambient temperature. In the literature, spin-state transitions are classified according to the shape of the magnetization curve<sup>3,16</sup> (complete, incomplete, one-step, two-step, multi-step with or without plateau, hysteresis or not) and according to the temperature range necessary for the complete change of the spin state: a spin state transition occurring over more than 10 K is termed gradual or continuous, and over fewer than 10 K, it is termed abrupt or discontinuous.<sup>16</sup> Systematic design of SCO-materials has, unfortunately, to date proven to be impossible. Several influences, often difficult to identify independently overlap, resulting in the observed spin state transition behavior. Among them, cooperativity – the transfer of volume-work due to the spin-state related elongation of the Fe–N bond by a rigid ligand – between the (inter) molecular alignment and crystal packing is commonly stated as a necessary ingredient for a complete and abrupt HS–LS spin state transition.<sup>17</sup> There are several ways to introduce cooperativity in SCO-materials, including guest molecules, co-crystallized solvents or the appropriate choice of the anion, whereby the density of the packing in the crystal and intermolecular interactions can be tuned.<sup>15,18,19</sup> Hydrogen-bonding networks have proven to be especially reliable tools sharpening the abruptness of the spin crossover behavior by enhancing cooperativity. Although, this seems to be the best prospective method for tuning SCO-behavior, relying on intermolecular interactions still requires lengthy trial and error investigations, since no unambiguous quantitative relationship between hydrogen-bonding parameters and SCO behavior is known.<sup>20,21</sup>

To suppress the unpredictable side-effects, based on earlier studies of homologous ligand series and design,<sup>22–24</sup> a ligand was designed which would promote the cooperativity of the system based on its structural features. A rigid and inelastic connection between single SCO-sites will directly transfer the

<sup>a</sup>Institute of Applied Synthetic Chemistry, TU Wien, Getreidemarkt 9/163-AC, 1060 Vienna, Austria. E-mail: danny.mueller@tuwien.ac.at

<sup>b</sup>Department of Mineralogy and Crystallography, University of Vienna, Althanstraße 14 (UZA 2), 1090 Vienna, Austria

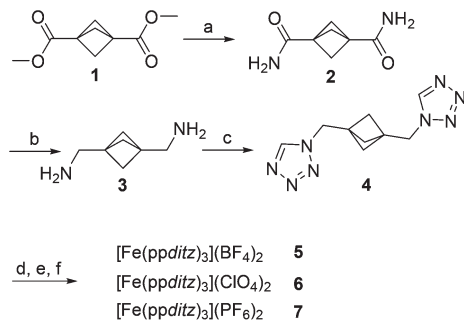
<sup>c</sup>Atominstytut, TU Wien, Stadionallee 2, 1020 Vienna, Austria

<sup>d</sup>X-Ray Center, TU Wien, Getreidemarkt 9, 1060 Vienna, Austria

<sup>e</sup>Institute of Solid State Physics, TU Wien, Wiedner Hauptstraße 8-10/138, 1040 Vienna, Austria

† Electronic supplementary information (ESI) available: Experimental details for all new compounds, and spectroscopy characterization of all new compounds. 1564873 (5, HS), 1564874 (5, LS), 1564875 (6, HS), and 1564876 (6, LS). For ESI and crystallographic data in CIF or other electronic format see DOI: 10.1039/c8dt00781k





**Scheme 1** Synthesis of compounds 1–7. (a)  $\text{NH}_3$  (b)  $\text{LiAlH}_4$  (c)  $\text{NaN}_3$ , triethyl orthoformate, acetic acid (d)  $\text{Fe}(\text{BF}_4)_2 \cdot 6\text{H}_2\text{O}$  (e)  $\text{Fe}(\text{ClO}_4)_2 \cdot 6\text{H}_2\text{O}$  (f)  $\text{Fe}(\text{PF}_6)_2$ .

volume work associated with the spin state transition more efficiently than probably realized by intermolecular interactions, thus establishing cooperativity in the system.<sup>3,25</sup> Combining internal rigidity with a bridging coordination template which could avoid large, solvent-incorporating cavities, should promote abrupt and cooperative SCO behavior. Based on these assumptions, the 1,3-bis((1*H*-tetrazol-1-yl)methyl) bicyclo[1.1.1]pentane (ppditz) ligand, including a highly strained propellane spacer as a short, rigid linker between the coordinating  $\text{CH}_2$ -tetrazole moieties, was synthesized (Scheme 1).

The reaction of ppditz (4) with  $\text{FeX}_2$  ( $\text{X} = \text{BF}_4^-$ ,  $\text{ClO}_4^-$ ,  $\text{PF}_6^-$ ) resulted in the corresponding  $\text{Fe}(\text{II})$ -SCO complexes 5, 6 and 7 (Scheme 1), as beige solids at ambient temperature and bright magenta when cooled in liquid nitrogen.

The quantification of the temperature dependent magnetic susceptibility for 5–7 shows a change in the magnetic moment from  $3.55 \text{ cm}^3 \text{ K mol}^{-1}$  to  $0.47 \text{ cm}^3 \text{ K mol}^{-1}$ , characteristic of the change from an  $\text{Fe}^{2+}$  from a  $(t_{2g})^4(e_g)^2$  HS-state to a  $(t_{2g})^6$  LS-state in the octahedral ligand field (Fig. 1). The magnetization curves of the  $[\text{Fe}(\text{ppditz})_3]^{2+}$  cation with all three anions show an abrupt, single-step spin state transition with  $T_{1/2}$  between 170 K (7,  $\text{PF}_6^-$ ), and 187 K (6,  $\text{ClO}_4^-$ ).  $[\text{Fe}(\text{ppditz})_3](\text{BF}_4)_2$  (5) shows the sharpest transition of the series ( $T_{1/2} = 173 \text{ K}$ ). The abrupt change in the temperature dependent magnetic moments of 5–7 verifies the initial assumption that the introduction of a rigid, highly strained linker between the coordinating tetrazole-moieties should result in an abrupt SCO. The curves in Fig. 1 demonstrate, that, in this case, the size ( $\text{BF}_4^-$  49 Å<sup>3</sup>;  $\text{ClO}_4^-$  54 Å<sup>3</sup>;  $\text{PF}_6^-$  69 Å<sup>3</sup>) and geometry (tetrahedral vs. octahedral) of the weakly-coordinating anion has only a minimal influence on the SCO, shifting slightly the  $T_{1/2}$ -values in the series. For all samples, the magnetic susceptibilities on both cooling and heating were identical (see Fig. S1–S3†). The SCO-correlated change in the absorption of light by the materials was monitored by variable temperature UV-VIS/NIR spectroscopy (Fig. S4–S6†), all three materials show a maximum for the HS complex around 865 nm ( $^5\text{T}_2 \rightarrow ^5\text{E}$ ) and at 550 nm for the LS complex ( $^1\text{A}_1 \rightarrow ^1\text{T}_1$ ). In the MIR-spectra the tetrazolic  $\nu_{\text{CH}}$  and  $\nu_{\text{NN}}$  are shifted by 4–9  $\text{cm}^{-1}$ , corresponding to the decreasing interatomic distance on tran-

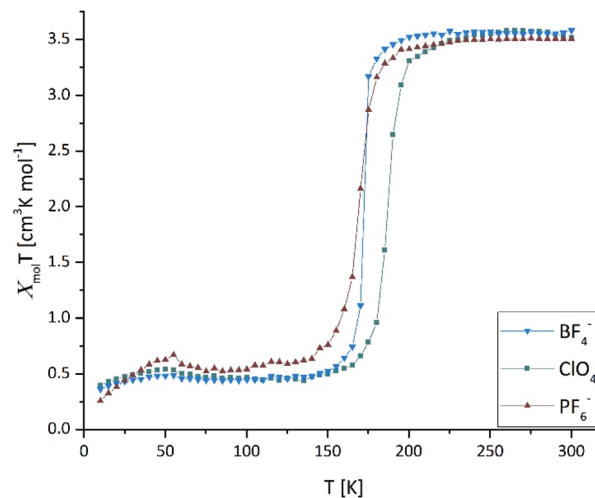


**Fig. 1** Magnetic susceptibility of  $[\text{Fe}(\text{ppditz})_3]\text{X}_2$ ,  $\text{X} = \text{BF}_4^-$ ,  $\text{ClO}_4^-$ , and  $\text{PF}_6^-$  in the solid state between 10 K–300 K.

sition from the HS to the LS-state (Fig. S7, S9 and S11†).<sup>26,27</sup> In the FIR spectra of all three compounds (Fig. S8, S10 and S12†) a distinct spin-state dependent iron motion against the N–N–N-planes in the  $\text{N}_6$ -octahedron for the LS-state is observed at  $252 \text{ cm}^{-1}$ . The corresponding vibrational mode for the iron motion in the HS-state cannot be unambiguously attributed to a single spectral feature, as it coincides with several vibrational modes of the propellane-spacer and the iron motion has no longer been the main contributor (see Fig. S21†).<sup>26,27</sup>

Single crystals suitable for X-ray structural analysis of 5 and 6 were grown by layer-to-layer diffusion of the corresponding  $\text{Fe}(\text{II})$ -source and ppditz. For compound 7 no single crystals could be obtained, regardless of the crystallization conditions. The compounds crystallize in the trigonal space group  $P\bar{3}c1$ , forming 1-dimensional, infinite chains of cations along [001] with  $P\bar{3}1c$ -symmetry (Fig. S13†). The chains consist of a unique ppditz-ligand, bridging between two iron centers. Each iron atom is surrounded by six identical ppditz-ligands, coordinating to the iron by the N4-nitrogen. The formation of infinite, cationic, 1D-chains is characteristic for bidentate tetrazole ligands,<sup>22,23,28–30</sup> although, the ppditz-ligand used herein stands in contrast to literature known examples since it is devoid of flexibility. Both Fe–N bond-lengths and bond-angles are the same for all six coordinating ligands (Tables S1 and S2†). The Fe–N distances in the HS-state (2.187 Å, 5 and 2.179 Å, 6) and in the LS-state (2.020 Å, 5 and 2.026 Å, 6) are in good agreement with the values expected for  $\text{Fe}^{2+}$ -tetrazole SCO-complexes.<sup>3</sup> The channels between the ppditz-chains are occupied by the anions, yielding a non-porous structure (see Fig. S14†). Both tetrahedral anions are disordered in a pseudo mirror-symmetry with the mirror-plane parallel to (001) and are located at the Wyckoff Position 4d with a threefold symmetry. A remarkable feature of both structures of 5 and 6 is the complete absence of a stabilizing, intermolecular hydrogen bonding network. This minimizes any interaction between the



single  $[\text{Fe}(\text{ppditz})_3]^{2+}$  chains, as well as between the chains and the anions. This confines the cooperativity of the established structure to the infinite cationic chains. Due to the rigidity of the *ppditz*-linker between the coordinating tetrazoles, the volume-work caused by the extension of the Fe–N bond-lengths during the spin crossover is directly transferred to the adjacent Fe-centers. The ligand, bridging two iron centers each, is largely unaffected by the Fe(II)'s spin state, undergoing only slightest variation in the angle between the propellane-linker and the coordinating tetrazoles.

A comparison of both the HS and LS structures of **5** and **6** with representative distances and angles of the cavity is given in Fig. 2. The structural analysis provides a ready explanation for the slightly different magnetic behavior of **5** and **6** (a larger  $\text{ClO}_4^-$  anion results in a slightly more gradual transition with a 14 K higher  $T_{1/2}$  than the  $\text{BF}_4^-$  analogue). The presence of a slightly larger anion in the channels between the *ppditz*-chains ( $\text{ClO}_4^-$  in place of  $\text{BF}_4^-$ ) results in different structural changes compensating for the volume work during the spin crossover. In the case of the smaller  $\text{BF}_4^-$ , expansion occurs predominantly in the *xy*-plane, with a slight lengthening of the Fe–Fe distance along the *z*-axis (Table 1). In the case of the larger  $\text{ClO}_4^-$ , the Fe–Fe distance is increased nearly twice as much as in the  $\text{BF}_4^-$  case and the Fe–N bond-distance is elongated to a lesser degree (Table 1).

The small cavities between the three *ppditz*-ligands are unoccupied, as was confirmed by  $^1\text{H-NMR}$  (Fig. S15 $\dagger$ ) and thermogravimetry (Fig. S16–S18 $\dagger$ ). In no case was any evidence for incorporated solvent molecules in the structures found. Nonetheless, all four structures feature cavities occupied by small residual electron densities after refinement of the struc-

**Table 1** Elongation of bond-lengths and distances in **5** and **6** on spin crossover

	Elongation of the Fe–N bond-length [%]	Elongation of the Fe–Fe distance [%]
$\text{BF}_4^-$ ( <b>5</b> )	8.27	0.65
$\text{ClO}_4^-$ ( <b>6</b> )	7.55	1.29

tural models. The geometry of the residual peaks in these voids resembles a disordered, tetrahedral anion of low occupancy, located at the Wyckoff-position 2i, allowing for a tetrahedral occupation. Even using structural restraints, no stable refinement of atoms at these positions was possible. Therefore these residual electron densities were removed by using the Platon SQUEEZE-algorithm<sup>31</sup> to improve the overall quality of the refinement. Considering the electron density calculated by SQUEEZE (see Table S4 $\dagger$ ), approximately every 4<sup>th</sup> void is occupied by an anion in the case of structure **5**, whereas for **6** every 3<sup>rd</sup> void contains a disordered anion. Although, the anion incorporation in cavities between ligands is rather uncommon in SCO-materials, several notable examples of anion incorporation in other metal organic frameworks (MOFs) have been reported.<sup>32–35</sup>

To correlate the structural changes during the spin crossover in **5–7** with the magnetic measurement, temperature dependent powder X-Ray diffraction (P-XRD) was performed. The shift of the peak-positions originating from the volume-contraction/expansion during the change of the spin state observed in the P-XRD data (Fig. 3, Fig. S19 and S20 $\dagger$ ) correlates reasonably with the  $T_{1/2}$  derived from the susceptibility data. Based on the P-XRD data compounds **5–7** were verified to be isostructural.

To allow for a detailed assignment of experimental spectroscopy features and theoretically model the structural moiety of the SCO-material, a quantum chemical model based on  $[\text{Fe}(\text{ppditz})_3]^{2+}$ -chains was compared to the experimental data. For this purpose, DFT-calculations with the hybrid functional

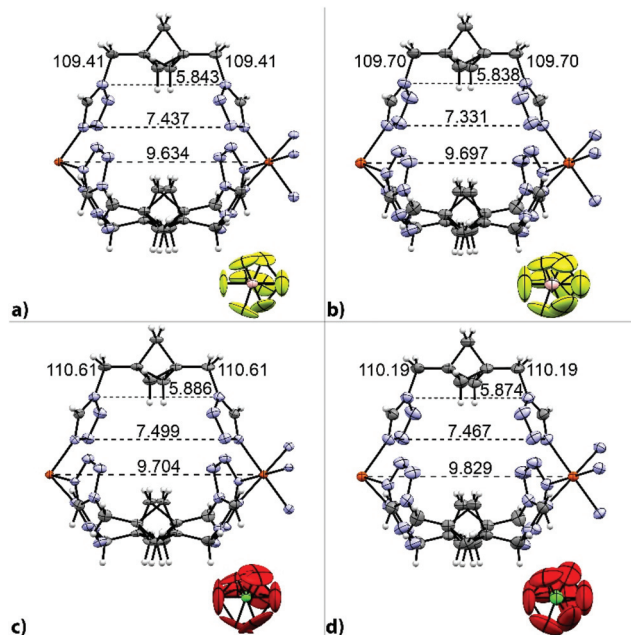


**Fig. 2** Single  $[\text{Fe}(\text{ppditz})_3]^{2+}$ -unit of **5** and **6** in the low-spin (left, a and c) and high-spin (right, b and d).

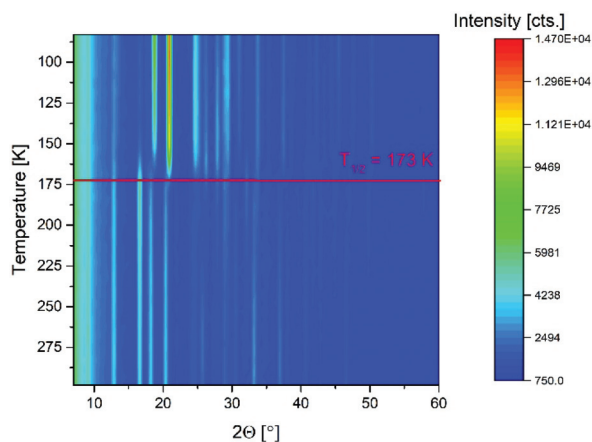


**Fig. 3** Waterfall-plot of the temperature-dependent P-XRD data of **5**. The spin crossover associated volume work is observed at 173 K due to the shift of the peak positions. The inserted line is meant as a guide for the eye (for P-XRD data of **6** and **7** see Fig. S19 and S20).



B3LYP<sup>36–38</sup> and the 6-311++g(d,p) valence triple zeta basis set<sup>39</sup> including polarization and diffuse functions on all atoms were used. The infinite cationic chains were approximated by two 1,3-bis((1*H*-tetrazol-1-yl)methyl)bicyclo[1.1.1]pentane moieties with a charge of +6 and a spin-multiplicity of 13 without anions in the gas phase, with methyl-tetrazole end groups. For comparison with experimental data only the bond lengths and bond angles of the inner iron(II) center were considered. The structural parameters and bond lengths are in good agreement with experimental findings, except for the Fe–Fe distance, which is overestimated by more than one angstrom (see Tables S5 and S6†). This deviation is known and can be attributed to the absence of the adjacent cationic chains present in the solid phase.<sup>26,40</sup> The N–Fe–N angles of the coordination octahedron correspond to the experimental findings, deviating only slightly from 90°. Regarding the spectroscopy features, the absolute, uncorrected values differ from the experimental findings, nevertheless the difference between the high spin and low spin state agrees with the experimentally observed shifts. Detailed investigation of the different calculated vibrational modes resulted in the identification of the above mentioned characteristic iron motion in the N<sub>6</sub>-octahedron for the LS-state,<sup>26</sup> representing the main contribution to the experimental FIR-band at 252 cm<sup>-1</sup> (see Fig. S21†).

In conclusion, 1,3-bis((1*H*-tetrazol-1-yl)methyl)bicyclo[1.1.1]pentane (ppditz) was chosen as a highly strained, rigid bridging ligand that decouples rigidity and cooperativity leading to an abrupt spin state transition from intermolecular influences. The success of this strategy was confirmed by the examination of three novel Fe(II)-SCO materials with different anions (BF<sub>4</sub><sup>-</sup>, ClO<sub>4</sub><sup>-</sup>, and PF<sub>6</sub><sup>-</sup>), all of which show an abrupt, single-step, complete and cooperative spin crossover between 170 K and 187 K. In the absence of intermolecular interactions, as demonstrated by structural characterization, the spin crossover is governed solely by the inherent inflexibility of the ligand itself. Of the effects known to govern SCO behavior (ligand flexibility, anion size, guest molecules present within the cavities, solvent effects and intermolecular interactions), all factors except the anion size were carefully controlled. The fact that the variation of the anion size had only a small impact on the resulting spin state transition shows that, in the present case, spin state transition is governed solely by the ligand properties. This study may act as a showcase example of structure–property based rational design of spin crossover materials with enhanced cooperativity.

## Conflicts of interest

There are no conflicts to declare.

## Acknowledgements

We acknowledge financial support of the Austrian Science Fund (FWF Der Wissenschaftsfond) project P 31076. The computational results presented have been achieved using the

Vienna Scientific Cluster, elemental analysis was performed at the Microanalytical Laboratory, Vienna University. Special thanks are to the X-ray center of TU Wien and Dr. Klaudia Hradil. This work was performed in the framework of the Corporation in Science and Technology (COST) action CM1305 “Explicit Control Over Spin-states in Technology and Biochemistry (ECOSTBio)”.

## Notes and references

- 1 A. Bousseksou, G. Molnar, L. Salmon and W. Nicolazzi, *Chem. Soc. Rev.*, 2011, **40**, 3313–3335.
- 2 P. Gütllich, *Eur. J. Inorg. Chem.*, 2013, 581–591.
- 3 P. Gütllich and H. A. Goodwin, *Topics in Current Chemistry*, Springer, Berlin Heidelberg, 2004.
- 4 O. Kahn and C. J. Martinez, *Science*, 1998, **279**, 44–48.
- 5 T. Mahfoud, G. Molnar, S. Cobo, L. Salmon, C. Thibault, C. Vieu, P. Demont and A. Bousseksou, *Appl. Phys. Lett.*, 2011, **99**, 053307.
- 6 L. Zhu, F. Zou, J. H. Gao, Y. S. Fu, G. Y. Gao, H. H. Fu, M. H. Wu, J. T. Lu and K. L. Yao, *Nanotechnology*, 2015, **26**, 315201.
- 7 A. C. Aragonès, D. Aravena, J. I. Cerdá, Z. Acís-Castillo, H. Li, J. A. Real, F. Sanz, J. Hihath, E. Ruiz and I. Díez-Pérez, *Nano Lett.*, 2016, **16**, 218–226.
- 8 C. Lefter, V. Davesne, L. Salmon, G. Molnár, P. Demont, A. Rotaru and A. Bousseksou, *Magnetochemistry*, 2016, **2**, 18.
- 9 C. Lefter, S. Rat, J. S. Costa, M. D. Manrique-Juárez, C. M. Quintero, L. Salmon, I. Séguy, T. Leichle, L. Nicu, P. Demont, A. Rotaru, G. Molnár and A. Bousseksou, *Adv. Mater.*, 2016, **28**, 7508–7514.
- 10 C. Lefter, R. Tan, J. Dugay, S. Tricard, G. Molnár, L. Salmon, J. Carrey, W. Nicolazzi, A. Rotaru and A. Bousseksou, *Chem. Phys. Lett.*, 2016, **644**, 138–141.
- 11 C. Faulmann, K. Jacob, S. Dorbes, S. Lampert, I. Malfant, M. L. Doublet, L. Valade and J. A. Real, *Inorg. Chem.*, 2007, **46**, 8548–8559.
- 12 M. D. Manrique-Juarez, S. Rat, F. Mathieu, D. Saya, I. Séguy, T. Leichlé, L. Nicu, L. Salmon, G. Molnár and A. Bousseksou, *Appl. Phys. Lett.*, 2016, **109**, 061903.
- 13 S. Decurtins, P. Gutlich, K. M. Hasselbach, A. Hauser and H. Spiering, *Inorg. Chem.*, 1985, **24**, 2174–2178.
- 14 S. Decurtins, P. Gutlich, C. P. Kohler and H. Spiering, *J. Chem. Soc., Chem. Commun.*, 1985, 430–432.
- 15 H. J. Shepherd, C. Bartual-Murgui, G. Molnar, J. A. Real, M. C. Munoz, L. Salmon and A. Bousseksou, *New J. Chem.*, 2011, **35**, 1205–1210.
- 16 C. P. Köhler, R. Jakobi, E. Meissner, L. Wiehl, H. Spiering and P. Gütllich, *J. Phys. Chem. Solids*, 1990, **51**, 239–247.
- 17 J. A. Real, A. B. Gaspar, V. Niel and M. C. Munoz, *Coord. Chem. Rev.*, 2003, **236**, 121–141.
- 18 Z. Arcis-Castillo, F. J. Munoz-Lara, M. C. Munoz, D. Aravena, A. B. Gaspar, J. F. Sanchez-Royo, E. Ruiz, M. Ohba, R. Matsuda, S. Kitagawa and J. A. Real, *Inorg. Chem.*, 2013, **52**, 12777–12783.





- 19 F. J. Munoz-Lara, A. B. Gaspar, M. C. Munoz, A. B. Lysenko, K. V. Domasevitch and J. A. Real, *Inorg. Chem.*, 2012, **51**, 13078–13080.
- 20 M. M. Dîrtu, A. Rotaru, D. Gillard, J. Linares, E. Codjovi, B. Tinant and Y. Garcia, *Inorg. Chem.*, 2009, **48**, 7838–7852.
- 21 C. J. Johnson, G. G. Morgan and M. Albrecht, *J. Mater. Chem. C*, 2015, **3**, 7883–7889.
- 22 A. Absmeier, M. Bartel, C. Carbonera, G. N. L. Jameson, P. Weinberger, A. Caneschi, K. Mereiter, J. F. Letard and W. Linert, *Chem. – Eur. J.*, 2006, **12**, 2235–2243.
- 23 A. Absmeier, M. Bartel, C. Carbonera, G. N. L. Jameson, F. Werner, M. Reissner, A. Caneschi, J. F. Letard and W. Linert, *Eur. J. Inorg. Chem.*, 2007, 3047–3054.
- 24 G. Aromí, L. A. Barrios, O. Roubeau and P. Gamez, *Coord. Chem. Rev.*, 2011, **255**, 485–546.
- 25 H. Banerjee, S. Chakraborty and T. Saha-Dasgupta, *Inorganics*, 2017, **5**, 47.
- 26 M. Valtiner, H. Paulsen, P. Weinberger and W. Linert, *Match Commun. Math. Comput. Chem.*, 2007, **57**, 749–761.
- 27 P. Weinberger and M. Grunert, *Vib. Spectrosc.*, 2004, **34**, 175–186.
- 28 C. M. Grunert, J. Schweifer, P. Weinberger, W. Linert, K. Mereiter, G. Hilscher, M. Müller, G. Wiesinger and P. J. van Koningsbruggen, *Inorg. Chem.*, 2004, **43**, 155–165.
- 29 M. Quesada, F. Prins, E. Bill, H. Kooijman, P. Gamez, O. Roubeau, A. L. Spek, J. G. Haasnoot and J. Reedijk, *Chem. – Eur. J.*, 2008, **14**, 8486–8499.
- 30 M. Weselski, M. Książek, J. Kusz, A. Białońska, D. Paliwoda, M. Hanfland, M. F. Rudolf, Z. Ciunik and R. Bronisz, *Eur. J. Inorg. Chem.*, 2017, **2017**, 1171–1179.
- 31 A. L. Spek, *Acta Crystallogr., Sect. C: Struct. Chem.*, 2015, **71**, 9–18.
- 32 B. Chen, L. Wang, F. Zapata, G. Qian and E. B. Lobkovsky, *J. Am. Chem. Soc.*, 2008, **130**, 6718–6719.
- 33 R. Custelcean and B. A. Moyer, *Eur. J. Inorg. Chem.*, 2007, **2007**, 1321–1340.
- 34 D. Liu, K. Lu, C. Poon and W. Lin, *Inorg. Chem.*, 2014, **53**, 1916–1924.
- 35 K. L. Wong, G. L. Law, Y. Y. Yang and W. T. Wong, *Adv. Mater.*, 2006, **18**, 1051–1054.
- 36 C. T. Lee, W. T. Yang and R. G. Parr, *Phys. Rev. B: Condens. Matter Mater. Phys.*, 1988, **37**, 785–789.
- 37 A. D. Becke, *J. Chem. Phys.*, 1993, **98**, 5648–5652.
- 38 P. J. Stephens, F. J. Devlin, C. F. Chabalowski and M. J. Frisch, *J. Phys. Chem.*, 1994, **98**, 11623–11627.
- 39 R. Ditchfie, D. P. Miller and J. A. Pople, *J. Chem. Phys.*, 1971, **54**, 4186–4193.
- 40 M. Seifried, C. Knoll, G. Giester, M. Reissner, D. Müller and P. Weinberger, *Magnetochemistry*, 2016, **2**, 1–13.

